

2018

Defining hard and soft tissue asymmetry using three dimensional CBCT analysis

<https://hdl.handle.net/2144/32947>

"Downloaded from OpenBU. Boston University's institutional repository."

BOSTON UNIVERSITY
HENRY M. GOLDMAN SCHOOL OF DENTAL MEDICINE

THESIS

**DEFINING HARD AND SOFT TISSUE ASYMMETRY USING THREE
DIMENSIONAL CBCT ANALYSIS**

by

MARISA REASON

BA, Vanderbilt University, 2011

D.M.D, University of Pennsylvania School of Dental Medicine, 2015

Submitted in partial fulfillment of the requirements for the degree of
Master of Science in Dentistry
In the Department of Orthodontics and Dentofacial Orthopedics

2018

Reader Approval Page

First Reader

Dr. David Briss, DMD, FRCD(C)

Clinical Director, Department of Orthodontics and Dentofacial
Orthopedics

Second Reader

Dr. Melih Motro, DDS

Clinical Instructor, Department of Orthodontics and Dentofacial
Orthopedics

Third Reader

Dr. Goli Parsi, DMD, MS

Clinical Instructor, Department of Orthodontics and Dentofacial
Orthopedics

ACKNOWLEDGEMENTS

Firstly, I would like to thank my mentor, Dr. Briss, who guided me through my research and always responded to my emails and text messages (sometimes frantic ones) with support and assistance. He reassured me throughout the process and was always willing to help.

I would like to thank Dr. Motro for also assisting me when I needed help focusing my project and for reviewing my work when I needed it. He kept me to my deadlines and his endless reminders to send in our thesis drafts helped me stay on my toes.

A special thank you to Dr. Will for her support and encouragement throughout residency. She was always available to answer my questions and listen to my concerns. Also, a large thank you to Dr. Alpdogan Kantarci, who was my first ever research mentor in 2010 during a summer research project. He continued to be supportive and present throughout my dental career and I am happy to be back working with him in Boston.

Thanks to my readers, my co-residents, and faculty members, for their thoughtful and inspiring words, and also for their amusing jokes to keep me laughing and smiling over the last three years.

Last, but not least, thanks to my family for their unconditional love, care, and continual support.

DEFINING HARD AND SOFT TISSUE ASYMMETRY USING THREE
DIMENSIONAL CBCT ANALYSIS

Marisa Reason

Boston University, Henry M Goldman School of Dental Medicine, 2018

Major Professor: Dr. David Briss, DMD, FRCD(C); Clinical Director,

Department of Orthodontics and Dentofacial Orthopedics

ABSTRACT

Introduction: Asymmetry is a common occurrence in the craniofacial bones of humans and as Orthodontists, facial esthetics are a major concern in our daily practice¹. However defining asymmetry often relies on a subjective perception or an index that is established using 2-dimensional photos². To this day, most of the studies provide an arbitrary number to define a subject as asymmetric, but to the best of our knowledge, no study has analyzed subject's hard and soft tissue to find out where asymmetries originate in 3-dimensions.

Objectives: The aims of the study are to 1) establish appropriate, reproducible soft tissue landmarks and their bony counterparts in CBCT images 2) evaluate the correlation between the skeletal and soft tissue landmarks 3) use the measurements to objectively define asymmetry.

Materials and Methods: Cone Beam Computed Tomography (CBCT) images of 60 human subjects seeking or undergoing orthodontic treatment (mean age=19.8 ± 11.6)

were selected from a CBCT repository. The DICOM files were imported into InVivoDental5.3 software (Anatomage™; San Jose, Calif.) for screening. Hard and soft tissue masks were created on all scanned images. Two groups were created using a symmetry index adapted from the method prescribed by Grammer and Thornhill²: symmetric (n=48, mean age 19.68) and asymmetric (n=12, mean age=19.92). 10 hard and soft tissue landmarks were identified on each scan in reference to established mid-sagittal, nasion-horizontal, and coronal planes. Linear measurements to the reference planes were recorded giving all landmarks an x-, y-, and z- coordinate. Differences in means and standard deviations of the symmetric and asymmetric groups were done using student t-tests or Wilcoxon rank sum test with a 5% significance level. Spearman correlations tests were done between hard and soft tissue landmarks in the symmetric and asymmetric groups respectively.

Results: The differences in the mean linear distances between the symmetric and the asymmetric groups in 14 hard and soft tissue points to their respective planes were found to be statistically significant: These points included Pog, Pog', Gn, Gn', GoRL, GoRL'. Spearman correlation test showed that the r-values for 15 hard and soft tissue pairs were statistically significant.

Conclusion: Statistical significant differences exist in the linear measurements between hard and soft tissue points when comparing symmetric and asymmetric subjects. When we begin to compare the three planes, we see that significant bony asymmetries exist that are not visible to the human eye in 2-dimensions. Therefore, to define asymmetry a 3-dimensional analysis is needed to view where hard and soft tissue asymmetries originate.

TABLE OF CONTENTS

ACKNOWLEDGEMENTS.....	iii
ABSTRACT.....	iv
TABLE OF CONTENTS.....	vi
LIST OF TABLES.....	vii
LIST OF FIGURES.....	viii
REVIEW OF THE LITERATURE.....	1
HYPOTHESIS AND OBJECTIVES.....	6
METHODOLOGY.....	7
Statistical Method.....	14
RESULTS.....	15
DISCUSSION.....	34
CONCLUSIONS.....	39
REFERENCES.....	40
List of Journal Title Abbreviations.....	48
CURRICULUM VITAE.....	49

LIST OF TABLES

Table 1. The skeletal reference planes.....	10
Table 2. Auxiliary Planes.....	11
Table 3. Description of skeletal landmarks (bilateral landmarks are noted with R/L).	12
Table 4. Description of Soft Tissue Landmarks.	13
Table 5. Descriptive statistics of the sample population.....	15
Table 6. Reliability Test.....	16-18
Table 7. Comparison of the Differences in Means of Hard and Soft Tissue Variables in the Mid-Sagittal Plane (* notates statistically significant).	19
Table 8. Comparison of the Differences in Means of Hard and Soft Tissue Variables in the Nasion-Horizontal Plane (* notates statistically significant).....	20
Table 9. Comparison of the Differences in Means of Hard and Soft Tissue Variables in the Coronal Plane (* notates statistically significant).....	21
Table 10. R-values for Hard and Soft Tissue Pairs in Symmetric and Asymmetric groups respectively (* notes statistically significant).	22-23

LIST OF FIGURES

Figure 1. CBCT scan orientation in axial, sagittal, and coronal sections.	9
Figure 2. Skeletal reference planes.	10
Figure 3. Skeletal auxiliary planes.	11
Figure 4. A-MS measurements in the symmetric and asymmetric group.	24
Figure 5. B-MS measurements in the symmetric and asymmetric group.	25
Figure 6. Gn-MS measurements in the symmetric and asymmetric group.	26
Figure 7. GoR-MS measurements in the symmetric and asymmetric group.	27
Figure 8. GoL-MS measurements in the symmetric and asymmetric group.	28
Figure 9. OrR-MS measurements in the symmetric and asymmetric group.	29
Figure 10. OrL-MS measurements in the symmetric and asymmetric group.	30
Figure 11. MZSR-MS measurements in the symmetric and asymmetric group.	31
Figure 12. MZSL-MS measurements in the symmetric and asymmetric group.	32
Figure 13. Pog-MS measurements in the symmetric and asymmetric group.	33

REVIEW OF THE LITERATURE

There has been long history of research to quantify the relationship between the skeletal structure of the skull and the overlying soft tissue of the face³. Although one's face changes with time, the ability to recognize a familiar face does not alter drastically⁴. This ability depends a great deal on the soft tissue that presents itself, but the most important factor of human facial structure is the underlying skeleton⁵. However, there is a clear correlation between the relief of the skull and the surface of the soft tissue, and this can be illustrated in the asymmetry of the face⁶⁻⁸.

Asymmetry is a common occurrence in the craniofacial bones of humans and as Orthodontists, facial esthetics are a major concern in our daily practice. Shah and Joshi refer to esthetics with regard to symmetry and balance which overall gives us facial equilibrium defined as a "correspondence in size, form and arrangement of facial landmarks on opposite sides of the median sagittal plane". That is, the right and left sides of the face should have the same structures while also being mirror images of each other⁹.

Although one would expect symmetry to be coincident with esthetics, literature has demonstrated that a certain degree of asymmetry will actually characterize an esthetically pleasing face as oppose to harming it³. While an esthetic face may seem "balanced" and symmetrical, many faces will actually show underlying skeletal asymmetry that is simply masked to a layperson's eye by the presence of soft tissue¹⁰. A study by Peck and Kataja looked at 52 male and female white adult subjects with esthetic faces, as determined by being beauty contest winners, professional models or stars. They

found that each one displayed asymmetry in one or more of the bilateral measurements made on posterior-anterior cephalograms (PA cephs)¹¹.

A similar study done by Shah and Joshi examined 43 subjects with a "harmonious and symmetrical face" and "normal occlusion" by means of PA cephs⁹. They also demonstrated statistically significant differences between the right and left sides of the face, much like the cephalometric studies of Harvold, Shore, Mulick, Letzer and Kronman and Vig and Hewitt⁵⁻⁸. Moreover, they demonstrated that the overall right facial structure was larger than the left, consistent with findings from a study of Woo, in which it was hypothesized that this may be due to the presence of a larger right hemisphere of the brain causing an asymmetry in the cranial bones¹². Bjork also stated that in normal crania, there is a tendency for the bones on the right side to be larger than those on the left¹³. On the contrary, some studies have found structures on the left side to be larger than those on the right while others have failed to detect any sidedness^{4,8}. However, despite the existence of underlying skeletal asymmetry, studies by Fisher, Shah and Joshi found no influence or interference in establishing ideal occlusion^{2,9}. There seems to be a general consensus among researchers that varying amounts of asymmetry in craniofacial structures are a common finding, with unpredictable clinical impact.

Therefore, it is accepted that most faces in actuality are asymmetrical and this holds true among different cultures and nationalities. In fact, asymmetry is visible in fetuses as early as fourteen days in utero³. However, humans are often unaware of the asymmetry, and facial expression and head position can make asymmetries less conspicuous. Severt and Proffit found that the frequencies of a clinically apparent asymmetry in the human population were 5% in the upper face, 36% in the middle face,

and 74% in the lower face respectively¹⁴. Moreover, Bishara suggested that right and left differences would occur wherever there are two congruent, mirror image types. He claims that perfect bilateral symmetry is largely a theoretic concept and not actually found in nature¹⁵. If this is true, both hard and soft tissue should demonstrate some degree of asymmetry, even in a face that appears symmetric. However, Peck and Peck, who evaluated bilateral facial symmetry in white adults selected based on facial esthetics, concluded in their study that there is more stability and less asymmetry approaching the cranium and its components¹⁶. Another study looking at craniofacial asymmetry was performed using submental-vertical (SMV) radiographs from 44 adult dental students. Paired and unpaired landmarks of the facial regions were related to a reference coordinate system. It was concluded that some degree of asymmetry was found in all landmarks¹⁷. Many of these were the original studies that began the investigation into craniofacial skeletal and soft tissue asymmetry using the tools that were available to them at the time. A common theme, and limitation, among these studies is the use of two-dimensional imaging to represent a three-dimensional structure.

More recently, a 3-D computed tomography (CT) evaluation using linear and angular measurements in patients with and without facial asymmetries have reported several interesting findings. One study, which evaluated facial asymmetry in patients with juvenile idiopathic arthritis, found that glabella had the lowest deviation from the midsagittal reference plane and soft tissue deviations were found to decrease closer to the neurocranium¹⁸. There are numerous methods and techniques that can be used to evaluate craniofacial asymmetry, with different advantages and disadvantages. These can include direct measurement on dry skulls, which is the oldest method, lateral and

posterior-anterior cephalogram analyses, panoramic radiographs, anthropometrics, stereophotogrammetry, or facial photography in combination with any of the aforementioned^{1, 19}. In the past, it was suggested that a combination of posterior-anterior, lateral and submentovertex views could provide a 3D image for evaluation. With the advent of three-dimensional technology, and its application in many aspects of dentistry, this is no longer necessary^{20,21,22}. Both computed tomography and more recently cone beam computed tomography (CBCT) are becoming more widely used for craniofacial and dental applications. With regard to structural analysis, identifying bilateral anatomic landmarks related to a reference centerline, has been found to be a suitable method for quantifying skull asymmetry²³.

While conventional imaging techniques can be excellent diagnostic tools and have traditionally been used in craniofacial studies, they are limited by their two-dimensional nature, head positioning error, magnification and lack of overall image accuracy due to overlap and superimposition of structures^{19,24}. Fewer studies have been done using three-dimensional imaging, in particular cone-beam computed tomography that will be used in this study. With the advent of this imaging modality, Orthodontists are more frequently using CBCT for diagnosis, treatment planning and case follow-up. Its many advantages include, but are not limited to, higher quality, greater accuracy and less radiation than conventional 3D imaging with spiral CT²⁵⁻³⁰. Without CBCT images of patients, it is impossible to objectively index patients according to their hard and soft tissue asymmetries in 3-dimensions. Grammer and Thornhill provided a symmetry index which used photographs of patients in 2-dimensions². Although their mathematical method

provides a way to view asymmetries in an objective manner, it only considers the mid-sagittal plane as well as only evaluating soft tissue asymmetries.

Previous studies have considered hard and soft tissue asymmetries using CBCT, but most have focused on either skeletal or soft tissue landmarks^{4,7}. These studies have provided us with some knowledge regarding facial asymmetry in three dimensions, but none have previously attempted to objectively quantify where asymmetries originate in three dimensions. Further, this study also will try to explain at what rate does the soft tissue follow the hard tissue asymmetries. Many reports have concluded that underlying craniofacial skeletal asymmetry exists, is normal and in majority of cases is masked by soft tissue and or other compensations, thus remaining undetected due to how minor it is. These studies, however, have largely been completed using a two-dimensional reconstruction of a three-dimensional structure.

This investigation will evaluate three-dimensional CBCT images from patients who are divided into two groups. Those patients who are symmetric and then those who display a soft tissue asymmetry to consider measurements using anatomical hard and soft landmarks in all three planes of space. An analysis of the location of these landmarks to reference planes will provide valuable baseline measurements to evaluate hard and soft tissue asymmetries and to evaluate where the asymmetry initiates. Furthermore, correlation tests will provide information on how hard and soft tissue points relate to one another in a 3-dimensional analysis.

HYPOTHESIS AND OBJECTIVES

The objectives of this study are to use three-dimensional CBCT images to establish appropriate and reproducible hard and soft tissue landmarks, to compare the linear measurements of the landmarks in symmetric and asymmetric subjects, and to evaluate the correlations between the hard and soft tissue landmarks. After collecting the data, we can use the measurements to begin to objectively define asymmetries. Also, by determining the measurement correlations between hard and soft tissue landmarks, we can discover how the soft tissue follows the hard tissue in symmetric and asymmetric subjects respectively. This will provide a set of data that can be used as reference for future studies.

The null hypothesis is that given a random sample of the population, there is no statistical significant difference in the location/linear distance between landmark pair positions in the left and right sides of facial skeleton and the soft tissue across 3-dimensional reference planes in symmetric and asymmetric patients. The alternative hypothesis is that in a random sample, statistically significant differences exist between hard and soft tissue point pair positions to 3-dimensional reference planes in symmetric and asymmetric patients.

METHODOLOGY

Our retrospective cross sectional study was approved by the Institutional Review Board (IRB) of Boston University Medical Campus (Protocol Number: H-35814). This study was conducted using previously approved CBCT repository (H-32515) that included images of human subject seeking or undergoing orthodontic treatment.

To determine the required sample size, a pilot study was conducted using twenty CBCT images (i-CAT, Imaging Sciences International, Hatfield, PA, USA) according to a standard protocol (120 kV, 5 mA, FOV 17x23 cm, voxel size 0.3mm, exposure time 7s). Based on 80% power, 0.05 alpha error and a mean difference of 89.22 mm³ (SD=8.3 mm³) between Pog-MS, the estimated sample needed was 60 images. The sixty subjects comprised of 22 males and 38 females, and the age range of the selected patients was from 15.6 to 60 years of age with a mean age of 19.8 ± 11.6.

In our cross-sectional study the patients were selected as they presented, in no particular pre-determined order. The 60 subjects analyzed for this study were selected irrespective of gender, age, ethnicity, and dental malocclusion. The patients whose images were used did not have any systemic disease, syndrome or craniofacial anomaly.

Two groups were formed according to the purposes of this study:

A. The "symmetric group" consists of 48 subjects (mean age=19.68)

B. The "asymmetric group" consists of 12 subjects (mean age=19.92)

The 60 CBCTs to be used in the study were indexed using an adaptation of the method described by Grammer and Thornhill². Screenshots taken of the soft tissue drape of all subjects were used. The method used 12 measuring points; points used included

outer eye corners (P1 and P2) and inner eye corners (P3 and P4). The points measuring the cheekbones (P5 and P6) were defined as the most left and most right pixel of the face on a horizontal line beneath the eyes. A comparable definition was made for the points measuring the nose: P7 and P8 describe the most right and most left point of the nose in the lower nose region. Jaw width (P9 and P10) was measured as face width at the y-coordinate of the mouth corners (P11 and P12).

Facial asymmetry was calculated as the sum of all differences between the midpoints of six horizontal lines connecting the following pairs of points: P1–P2, P3–P4, P5–P6, P7–P8, P9–P10, P11–P12. The midpoints of each line were calculated using the formula $(\text{left point} - \text{right point})/2 + \text{right point}$. On a perfectly symmetrical face all midpoints lie on the same vertical line and the sum of non-redundant midpoint differences is zero. 10% of the subjects were two times two weeks apart by the same investigator. The point locations had very high reliability: The correlation between the facial symmetries calculated from the points of was .80 ($p < .0001$).

All 60 CBCT DICOM files were imported into InVivoDental5.3 software (Anatomage™; San Jose, Calif) for imaging and screening purposes as described above. The software divides the screen into four views: axial, coronal, sagittal, and 3-D view. Orientation is depicted in Figure 1. All of the images were processed by the same operator. After installing each DICOM file, initial orientation was verified. Using the previously oriented scan and the 3D-analysis function in InVivoDental5.3 software, initial orientation was identified. A mask was created on the scan to establish the 3-D bony skeleton. A reconstructed soft tissue mask was then created. The soft tissue 3-D or

skeletal 3-D model can be hidden or presented. This established hard and soft tissue reconstructions in three views (coronal, axial, sagittal).

To establish a standardized orientation, three-dimensional reference planes were set for each scan. Before the construction of the planes, the Frankfurt Horizontal plane was defined as passing through Left and Right Porion and Right Orbitale. Each axis was established as follows: Mid-Sagittal Plane (x), Nasion Horizontal Plane (y) and Coronal Plane (z). Skeletal auxiliary planes were also established in order to accurately plot the soft tissue points. Tables 1 and 2 describe the skeletal reference and auxiliary planes and Figure 2 and 3 depict the planes.

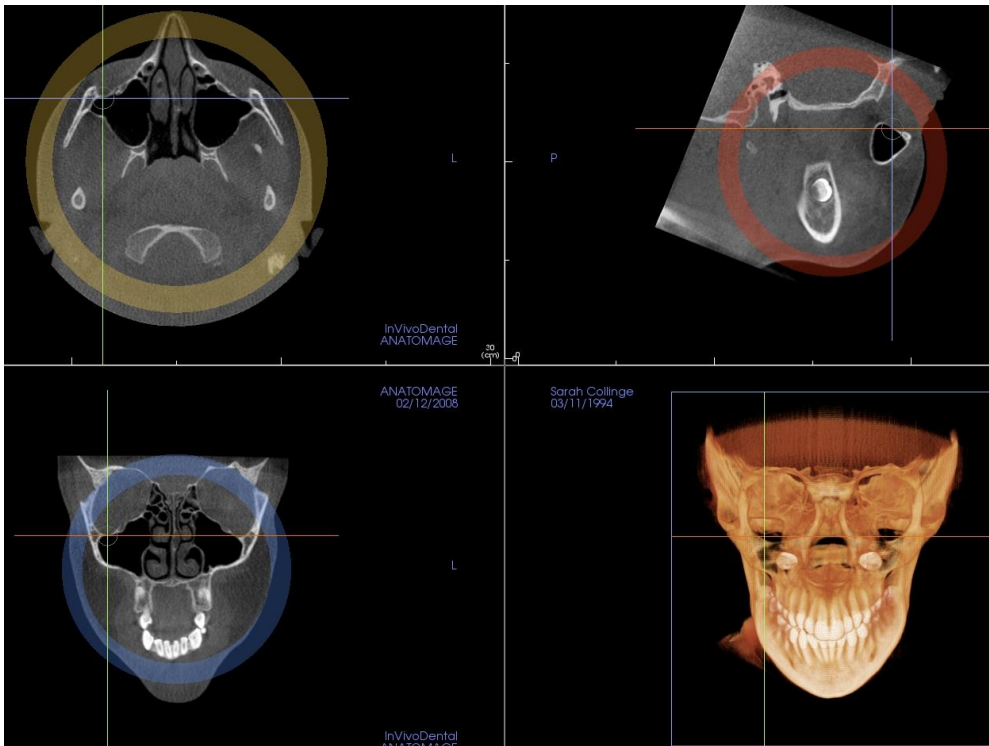


Figure 1. CBCT scan orientation in axial, sagittal, and coronal sections.

Table 1. The skeletal reference planes.

Mid-Sagittal Plane (MS, x-coordinate)	Passing through Basion and Nasion and being perpendicular to Nasion Horizontal Plane
Nasion Horizontal Plane (NH, y-coordinate)	Passing through Nasion parallel to Frankfort Horizontal-need to define
Coronal Plane (Cor, z-coordinate)	Passing through Basion and being perpendicular to the Nasion Horizontal Plane and Mid-Sagittal Plane

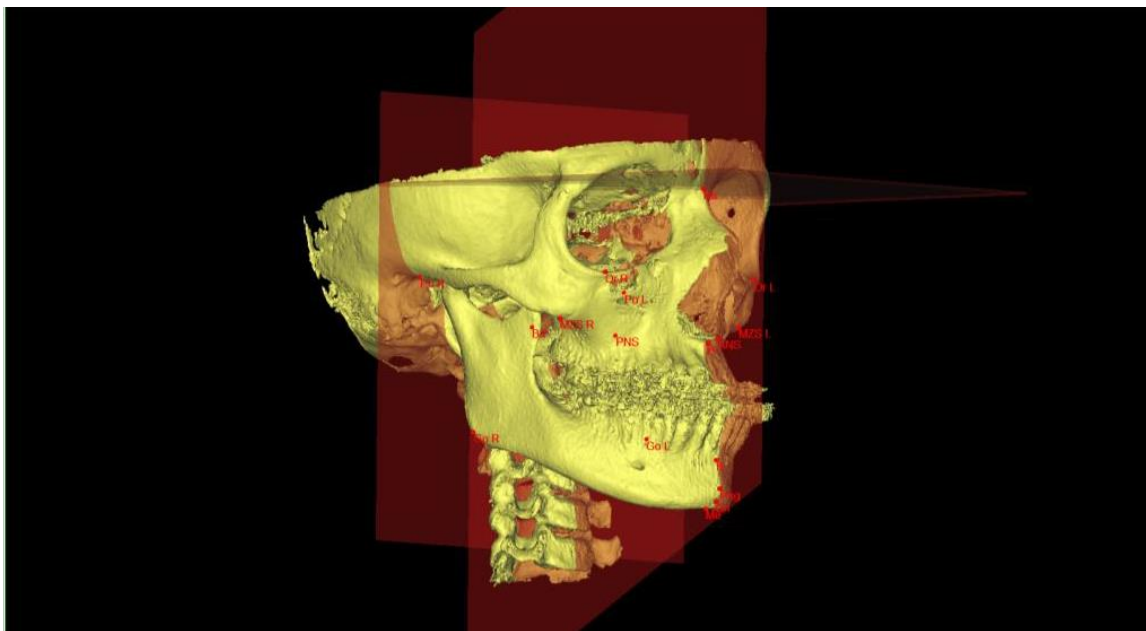


Figure 2. Skeletal reference planes.

Table 2. Auxiliary Planes.

Orbitale Horizontal Plane (OrH) (R/L)	Passing through Or (R/L) and parallel to FH
Orbitale Sagittal Plane (OrS) (R/L)	Passing through Or (R/L) and parallel to MS
Inferior-Maxillo-Zygomatic-Suture Horizontal Plane (MZSH (R/L)	Passing through MZS (R/L) and parallel to FH
Inferior-Maxillo-Zygomatic-Suture Sagittal Plane (MZSS) (R/L)	Passing through MZS (R/L) and parallel to MS
Gonion Horizontal Plane (GoH) (R/L)	Passing through Go (R/L) and parallel to FH
Gonion Coronal Plane (GoCor) (R/L)	Passing through Go (R/L) and parallel to Cor

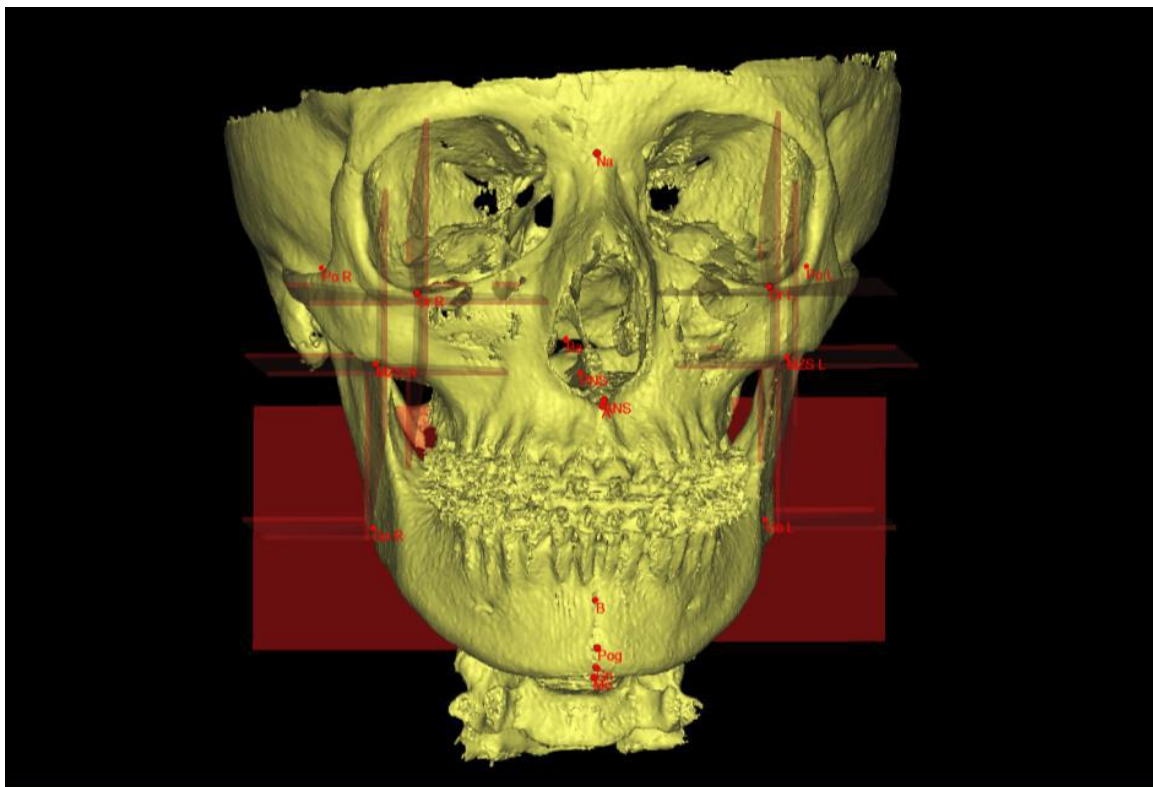


Figure 3. Skeletal auxiliary planes.

Based on a predefined cephalometrical analysis already described in the literature (Farkas 1994, Swennen et al 2005). 10 hard tissue soft tissue anatomic landmark points were used for analysis in this study. These are summarized and defined in Table 3 and Table 4. Landmarks were identified on each scan and individually verified in each plane to ensure accuracy of their three-dimensional location.

Table 3. Description of skeletal landmarks (bilateral landmarks are noted with R/L).

Landmark	Abbreviation	Description
A point	A	The deepest midline concavity on the maxilla between the anterior nasal spine and prosthion
B point	B	The deepest midline concavity on the mandibular symphysis between infradentale and pogonion
Pogonion	Pog	The most anterior point of the bony chin in the median plane
Gonion	Go (R/L)	The constructed point on the curvature of the mandibular angle by bisecting the angle formed by the ramus plane and the mandibular plane
Gnathion	Gn	The most anteroinferior point on the symphysis of the chin
Orbitale	Or (R/L)	The lowest point in the inferior margin of the orbit
Inferior Maxillo-Zygomatic Suture	MZS (R/L)	The most inferior point of maxilla zygomatic suture

Table 4. Description of Soft Tissue Landmarks.

Landmark	Abbreviation	Description
Soft tissue A point	A'	The most concave portion of the upper lip in the centerline
Soft tissue B point	B'	The most concave portion of the soft tissue chin outline in the centerline
Soft tissue Pogonion	Pog'	The most anterior midpoint of the chin
Gonion soft tissue	Go' (R/L)	The intersection of GoH and GoCor planes with the overlying cutaneous surface
Soft tissue Gnathion	Gn'	The most inferior midpoint on the soft tissue contour of the chin
Soft tissue Orbitale	Or' (R/L)	The intersection of OrH and OrS planes with the overlying cutaneous surface
Soft tissue Inferior Maxillo Zygomatic Suture	MZS' (R/L)	The intersection of MZSH and MZSS planes with the overlying cutaneous surface

InVivoDental5.3 software assigned each anatomic landmark a 3D coordinate, representing its location in all three planes of space. For example, A point could be represented as A(x,y,z). The total number of points used in this study was 20 and the number of measurements 120.

Statistical Method

Statistical calculations were performed with SAS 9.4 software (SAS Institute Inc., Cary, NC). Standard descriptive statistical calculations were done to calculate the mean and standard deviation of each landmark to its respective reference plane in both study groups. Also, Shapiro Wilk and Kolmogrov-Smirnov tests were done to determine the normal distribution of the data. If the variable was normally distributed a student t-test was performed; otherwise a Wilcoxon rank sum test was done with a 5% significance level. These tests were done to determine the differences of means and p-values of hard and soft tissue variables in each plane. Spearman correlations test were performed between hard and soft tissue landmarks in the symmetric and asymmetric groups respectively.

RESULTS

Descriptive statistics of the sample population were performed with the results summarized below in Table 5.

Table 5. Descriptive statistics of the sample population.

Parameter	Symmetry Group	Asymmetry Group
Gender (M/F)	(16/32)	(3/9)
	Mean/SD/Range	Mean/SD/Range
Age	19.68/9.8/15.6-60	19.92/11.2/15.6-60

Method of error was found to be within a 95% confidence interval for all the values measured. Intraclass Correlation Coefficient was found to be close to 0.9-1. All the measurements were found to be reliable. Reliability test results are found in Table 6.

Table 6. Reliability Test (continues on next page).

Intraclass Correlation Coefficient		95% Confidence Interval	
Lower Bound		Upper Bound	
A'-Cor	0.999	0.977	1.000
A'-NH	0.997	0.865	1.000
A'-MS	0.997	0.874	1.000
A-Cor	0.999	0.962	1.000
A-NH	1.000	0.994	1.000
A-MS	0.989	0.574	1.000
B'-Cor	0.998	0.928	1.000
B'-NH	1.000	0.997	1.000
B'-MS	0.997	0.888	1.000
B-Cor	0.998	0.910	1.000
B-NH	0.999	0.968	1.000
B-MS	0.934	0.559	0.998
Gn'-Cor	0.938	0.616	0.998
Gn'-NH	1.000	0.999	1.000
Gn'-MS	1.000	0.997	1.000
Gn-Cor	0.988	0.542	1.000
Gn-NH	0.997	0.881	1.000
Gn-MS	1.000	1.000	1.000
Go L-Cor	1.000	0.987	1.000
Go L-NH	0.999	0.946	1.000
Go L-MS	0.999	0.978	1.000
Go R-Cor	0.998	0.903	1.000
Go R-NH	0.997	0.877	1.000
Go R-MS	1.000	1.000	1.000
Go' L-Cor	1.000	0.998	1.000

Table 6. Reliability Test (continues on next page).

Intraclass Correlation Coefficient		95% Confidence Interval	
Lower Bound		Upper Bound	
Go' L-NH	0.998	0.940	1.000
Go' L-MS	1.000	0.991	1.000
Go' R-Cor	0.996	0.829	1.000
Go' R-NH	0.999	0.978	1.000
Go' R-MS	0.999	0.975	1.000
MZS L-Cor	0.997	0.901	1.000
MZS L-NH	0.999	0.964	1.000
MZS L-MS	0.999	0.976	1.000
MZS R-Cor	0.999	0.961	1.000
MZS R-NH	0.998	0.928	1.000
MZS R-MS	1.000	0.998	1.000
MZS' L-Cor	0.964	0.617	0.999
MZS' L-NH	1.000	0.984	1.000
MZS' L-MS	0.998	0.926	1.000
MZS' R-Cor	0.999	0.947	1.000
MZS' R-NH	0.998	0.905	1.000
MZS' R-MS	0.998	0.935	1.000
Or L-Cor	1.000	0.985	1.000
Or L-NH	0.950	0.937	0.999
Or L-MS	0.996	0.847	1.000
Or R-Cor	0.999	0.942	1.000
Or R-NH	1.000	0.996	1.000
Or R-MS	1.000	0.994	1.000
Or' L-Cor	0.999	0.966	1.000
Or' L-NH	0.997	0.884	1.000
Or' L-MS	0.994	0.761	1.000

Table 6. Reliability Test (continued from previous page).

Intraclass Correlation Coefficient		95% Confidence Interval	
Lower Bound		Upper Bound	
Or' R-Cor	0.999	0.959	1.000
Or' R-NH	0.998	0.941	1.000
Or' R-MS	0.877	0.796	0.997
Pog'-Cor	1.000	0.998	1.000
Pog'-NH	0.975	0.733	0.999
Pog'-MS	1.000	0.997	1.000
Pog-Cor	0.999	0.948	1.000
Pog-NH	0.995	0.808	1.000
Pog-MS	0.877	0.796	0.997

After determining whether the variable showed normal distribution, a student t-tests or Wilcoxon rank sum test was performed with a 5% significance level or a p value of 0.05. Tables 7, 8, 9 show the results of these statistical tests.

Table 7. Comparison of the Differences in Means of Hard and Soft Tissue Variables in the Mid-Sagittal Plane (* notates statistically significant).

Variable	Symmetric		Asymmetric			Mean Difference (SD)
	Mean	SD	Mean	SD	P value	
A-MS	45.81	5.93	44.94	4.26	0.42	.87 (5.64)
B -MS	55.01	9.25	58.62	9.23	0.19	3.61 (9.24)
Gn-MS	58.78	4.34	57.36	3.39	0.3	1.42 (4.18)
GoR-MS	90.79	7.63	86.48	6.49	0.08	4.27 (7.43)
GoL-MS	90.62	7.51	89.72	4.79	0.66	.90 (7.07)
OrR-MS	81.4	5.85	79.48	5.69	0.19	1.93 (5.81)
OrL-MS	81.15	5.69	79.32	4.1	0.54	1.84 (5.42)
MZsR-MS	68.9	5.59	68.84	8.67	0.62	.06 (6.29)
MZsL-MS	68.91	5.51	66.39	6.56	0.29	2.52 (5.73)
Pog-MS	89.02	8.17	101.42	4.15	<.0001*	12.40 (7.57)
A'-MS	45.65	6.07	44.92	5.59	0.42	.73 (5.98)
B'-MS	54.59	8.25	64.25	5.54	0.31	9.67 (7.81)
Gn'-MS	58.83	4.32	57.17	4.02	<.0001*	1.66 (4.26)
GoR'-MS	90.77	7.73	68.05	5.61	<.0001*	22.71 (7.37)
GoL'-MS	90.96	7.78	67.31	5.51	<.0001*	23.65 (7.40)
OrR'-MS	81.34	5.81	80.01	3.78	0.72	1.33 (5.48)
OrL'-MS	81.41	6.02	79.31	3.57	0.44	2.11 (5.64)
MZsR'-MS	68.84	5.71	72.52	5.84	0.06	3.68 (5.73)
MZsL'-MS	68.87	5.69	69.92	7.71	0.84	1.04 (6.12)
Pog'-MS	92.36	6.83	88.1	3.99	0.008*	4.26 (6.39)

Table 8. Comparison of the Differences in Means of Hard and Soft Tissue Variables in the Nasion-Horizontal Plane (* notates statistically significant).

Variable	Symmetric		Asymmetric			Mean Difference (SD)
	Mean	SD	Mean	SD	P value	
A-NH	81.77	5.41	86.51	5.68	0.12	4.74 (5.46)
B-NH	53.64	7.82	52.58	6.15	0.62	1.06 (7.53)
Gn-NH	74.03	6.04	83.24	9.03	0.005*	9.21 (6.71)
GoR-NH	78.62	10.2	86.99	4.38	<.0001*	8.36 (9.38)
GoL-NH	78.66	10.08	86.53	3.89	0.004*	7.87 (9.22)
OrR-NH	82.08	8.41	83.85	8.42	0.32	1.77 (8.41)
OrL-NH	82.27	8.48	83.91	8.11	0.54	1.64 (8.41)
MZsR-NH	54.62	7.87	56.47	9.19	0.49	1.85 (8.13)
MZsL-NH	54.72	7.85	58.63	8.68	0.18	3.91 (8.01)
Pog-NH	87.54	7.22	77.25	8.32	0.0013	10.29 (7.44)
A'-NH	80.92	4.81	78.22	6.35	0.08	2.74 (5.14)
B'-NH	51.19	7.93	56.16	4	0.06	4.97 (7.34)
Gn'-NH	74.61	6.69	65.52	4.82	<.0001*	9.09 (6.381)
GoR'-NH	82.28	6.69	83.83	8.55	0.73	1.55(7.09)
GoL'-NH	82.49	6.77	84.44	8.85	0.61	1.94 (7.21)
OrR'-NH	86.44	9.56	91.62	5.55	0.1	5.19 (8.94)
OrL'-NH	86.59	9.74	92.24	4.71	0.06	5.64 (9)
MZSR'-NH	58.25	6.79	54.18	8.44	0.09	1.48 (7.08)
MZsL'-NH	58.1	6.9	56.61	7.84	0.54	1.03 (6.26)
Pog'-NH	90.6	5.81	95.75	7.93	.13	5.15 (6.2)

Table 9. Comparison of the Differences in Means of Hard and Soft Tissue Variables in the Coronal Plane (* notates statistically significant).

Variable	Symmetric		Asymmetric			Mean Difference (SD)
	Mean	SD	Mean	SD	P value	
A-Cor	53.82	6.43	56.97	5.14	0.08	3.14 (6.21)
B-Cor	52.71	8.97	58.08	7.04	0.06	5.37 (8.63)
Gn-Cor	89.77	7.59	86.9	6.55	0.28	2.87 (7.4)
GoR-Cor	73.9	8.22	68.85	7.32	0.05	5.05 (8.06)
GoL-Cor	74.1	8.13	69.67	7.03	0.07	4.43 (7.93)
OrR-Cor	88.51	7.02	85.91	5.36	0.39	2.6 (6.73)
OrL-Cor	88.9	7.04	85.85	5.15	0.21	3.05 (6.73)
MZsR-Cor	53.22	9.34	54.505	7.2	0.61	1.28(8.97)
MZsL-Cor	53.59	9.51	54.77	6.88	0.63	1.18(9.07)
Pog-Cor	81.47	9	54.7	13.34	<.0001*	26.77 (9.97)
A'-Cor	55.66	9.19	61.44	4.61	0.07	5.78 (8.52)
B'-Cor	89.32	7.38	85.24	6.2	0.09	4.08 (7.17)
Gn'-Cor	76.14	10.54	80.57	3.52	0.03*	4.42(9.61)
GoR'-Cor	75.43	13.33	97.95	9.34	<.0001*	22.51 (12.67)
GoL'-Cor	75.48	13.26	100.46	4.89	<.0001*	24.98 (12.12)
OrR'-Cor	59.82	9.39	62.64	15.27	0.24	2.82 (10.75)
OrL'-Cor	59.83	9.43	63.46	16.47	0.21	3.62 (11.11)
MZSR'-Cor	49.67	8.64	56.79	5.8	0.08	7.13(8.18)
MZsL'-Cor	49.85	8.55	56.81	5.47	0.07	6.95(8.05)
Pog'-Cor	89.84	7.28	105.1	5.68	<.0001*	15.27(7)

Spearman correlation coefficients for the hard and soft tissue respective measurements are found in Table 10.

Table 10. R-values for Hard and Soft Tissue Pairs in Symmetric and Asymmetric groups respectively (* notes statistically significant) (continues on next page).

Variable		Symmetric		Asymmetric	
Hard Tissue	Soft Tissue	Rs-value	P-value	Rs-value	P-value
A-MS	A'-MS	0.96	<.0001*	-0.147	0.65
B-MS	B'-MS	0.99	<.0001*	-0.27	0.4
Gn-MS	Gn'-MS	0.98	<.0001*	0.07	0.82
GoR-MS	GoR'-MS	0.97	<.0001*	-0.07	0.82
GoL-MS	GoL'-MS	0.95	<.0001*	-0.21	0.52
OrR-MS	OrR'-MS	0.95	<.0001*	0.01	0.96
OrL-MS	OrL'-MS	0.92	<.0001*	0.17	0.6
MZsR-MS	MZsR'-MS	0.98	<.0001*	-0.21	0.52
MZsL-MS	MZsL'-MS	0.98	<.0001*	0.26	0.4
Pog-MS	Pog'-MS	-0.22	0.13	0.19	0.56
A-NH	A'-NH	0.1	0.49	0.8	0.002*
B-NH	B'-NH	0.42	0.77	-0.46	0.13
Gn-NH	Gn'-NH	0.76	0.04*	-0.23	0.48
GoR-NH	GoR'-NH	0.323	0.03*	-0.19	0.54
GoL-NH	GoL'-NH	0.33	0.02*	-0.09	0.78
OrR-NH	OrR'-NH	0.25	0.07	-0.36	0.24
OrL-NH	OrL'-NH	0.27	0.06	-0.09	0.77
MZsR-NH	MZSR'-NH	0.11	0.45	0.31	0.31
MZsL-NH	MZsL'-NH	0.17	0.25	0.122	0.7
Pog-NH	Pog'-NH	0.064	0.67	-0.36	0.244

Table 10. R-values for Hard and Soft Tissue Pairs in Symmetric and Asymmetric groups respectively (* notes statistically significant) (continued from previous page).

Variable		Symmetric		Asymmetric	
Hard Tissue	Soft Tissue	Rs-value	P-value	Rs-value	P-value
A-Cor	A'-Cor	0.38	0.12	0.52	0.08
B-Cor	B'-Cor	0.12	0.48	0.29	0.35
Gn-Cor	Gn'-Cor	0.18	0.2	-0.196	0.54
GoR-Cor	GoR'-Cor	-0.42	0.003*	-0.53	0.08
GoL-Cor	GoL'-Cor	-0.4	0.004*	-0.37	0.24
OrR-Cor	OrR'-Cor	0.08	0.58	0.56	0.06
OrL-Cor	OrL'-Cor	0.16	0.26	0.32	0.31
MZsR-Cor	MZSR'-Cor	0.05	0.74	-0.15	0.64
MZsL-Cor	MZsL'-Cor	0.03	0.84	-0.13	0.68
Pog-Cor	Pog'-Cor	-0.15	0.3	-0.18	0.57

To better visualize the comparisons of the symmetric and asymmetric measurements, graphical overlays were done depicting the measurement comparisons of each skeletal point in the MS plane. Figures 4-13 represent the graphical distribution of the linear measurements to the mid-sagittal reference between the symmetric and asymmetric group. The x-axis represents the measurements and the y-axis is the percentage of each subject. Blue represents the symmetrical group and red represents the asymmetrical group.

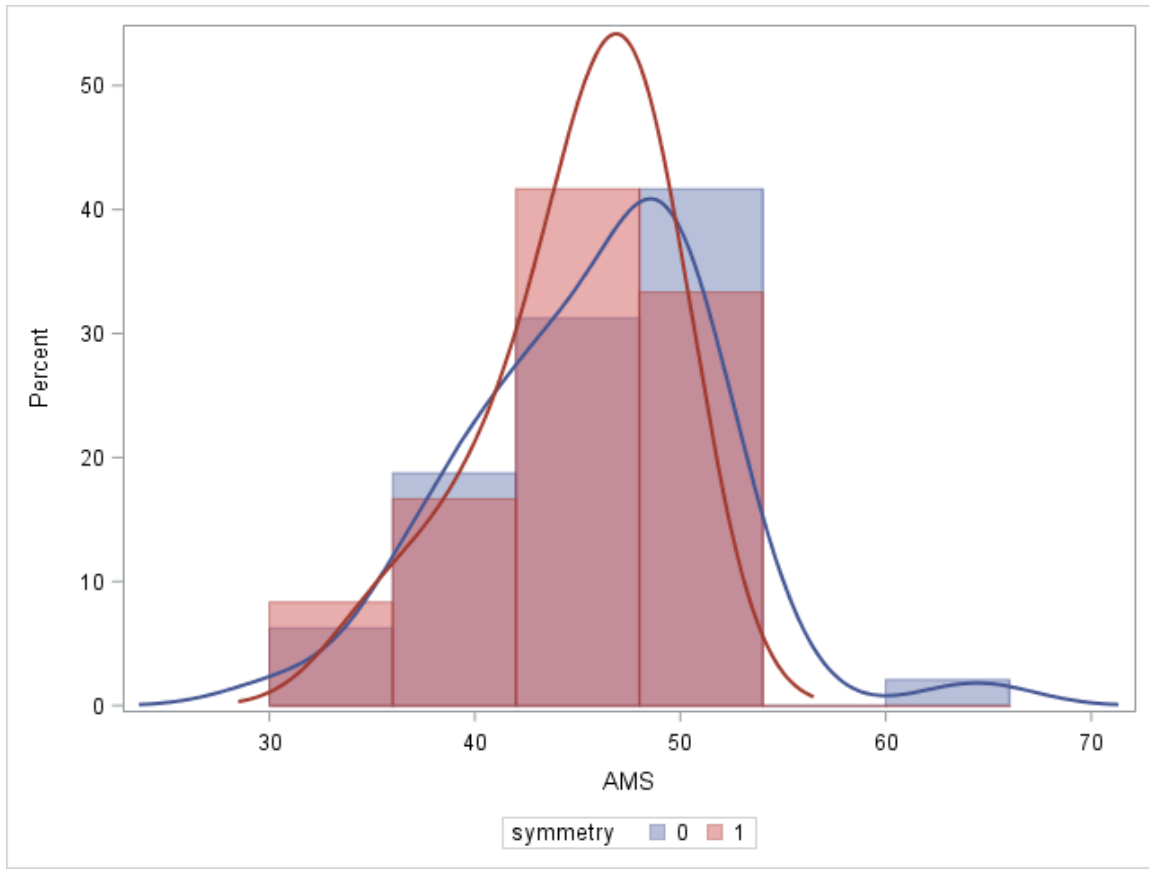


Figure 4. A-MS measurements in the symmetric and asymmetric group.

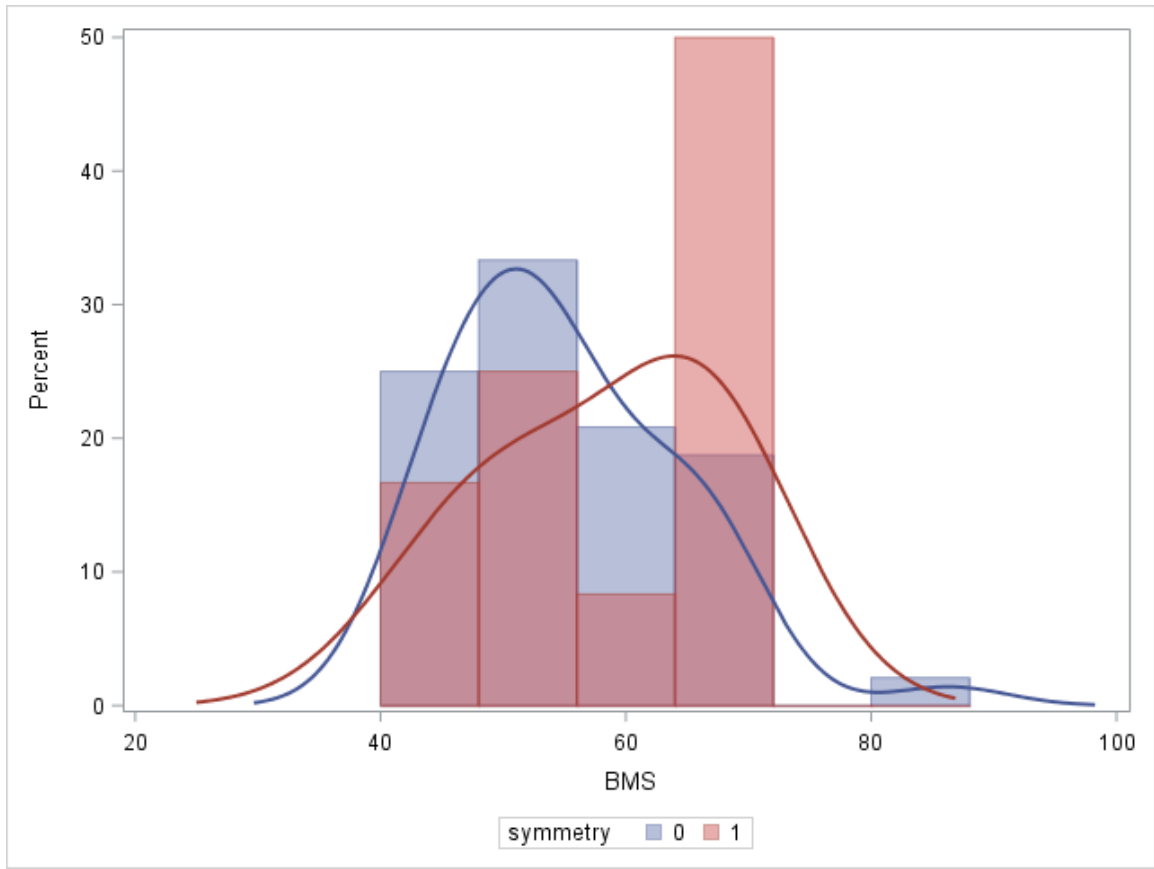


Figure 5. B-MS measurements in the symmetric and asymmetric group.

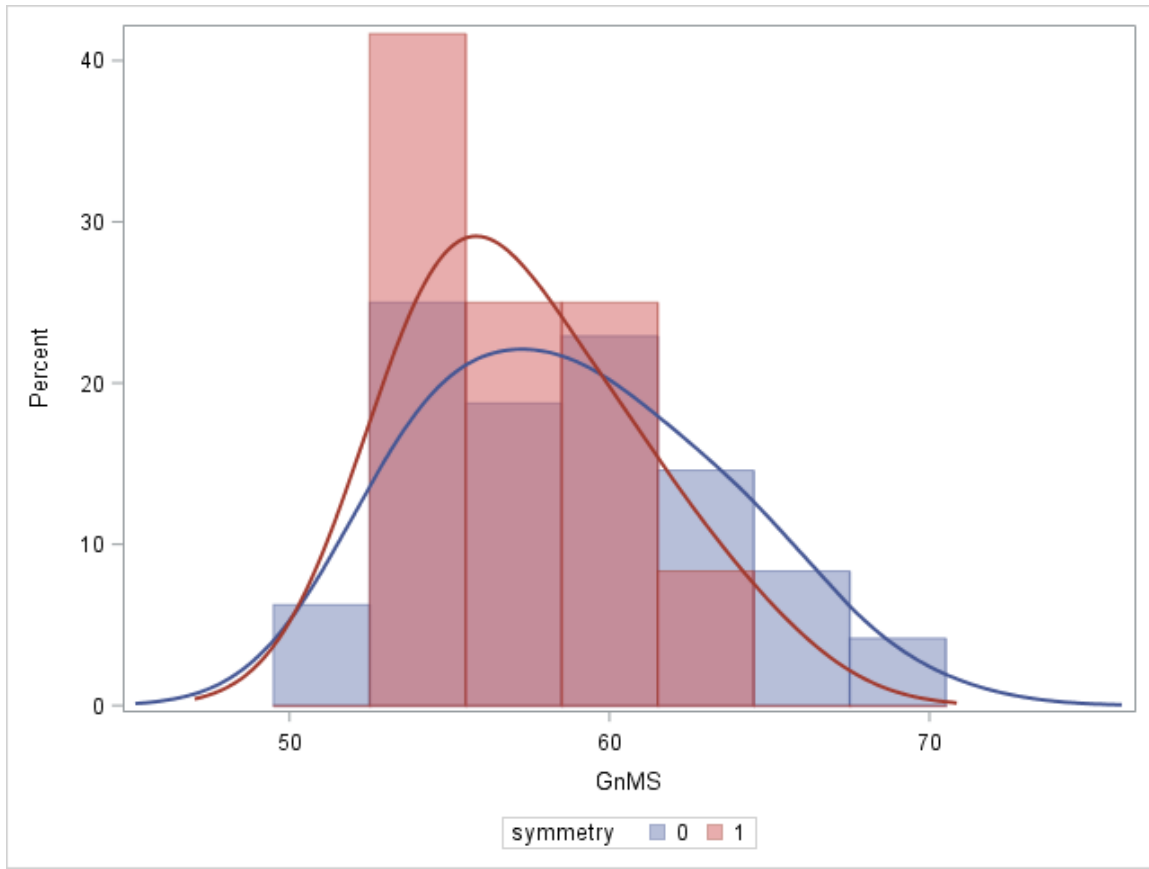


Figure 6. Gn-MS measurements in the symmetric and asymmetric group.

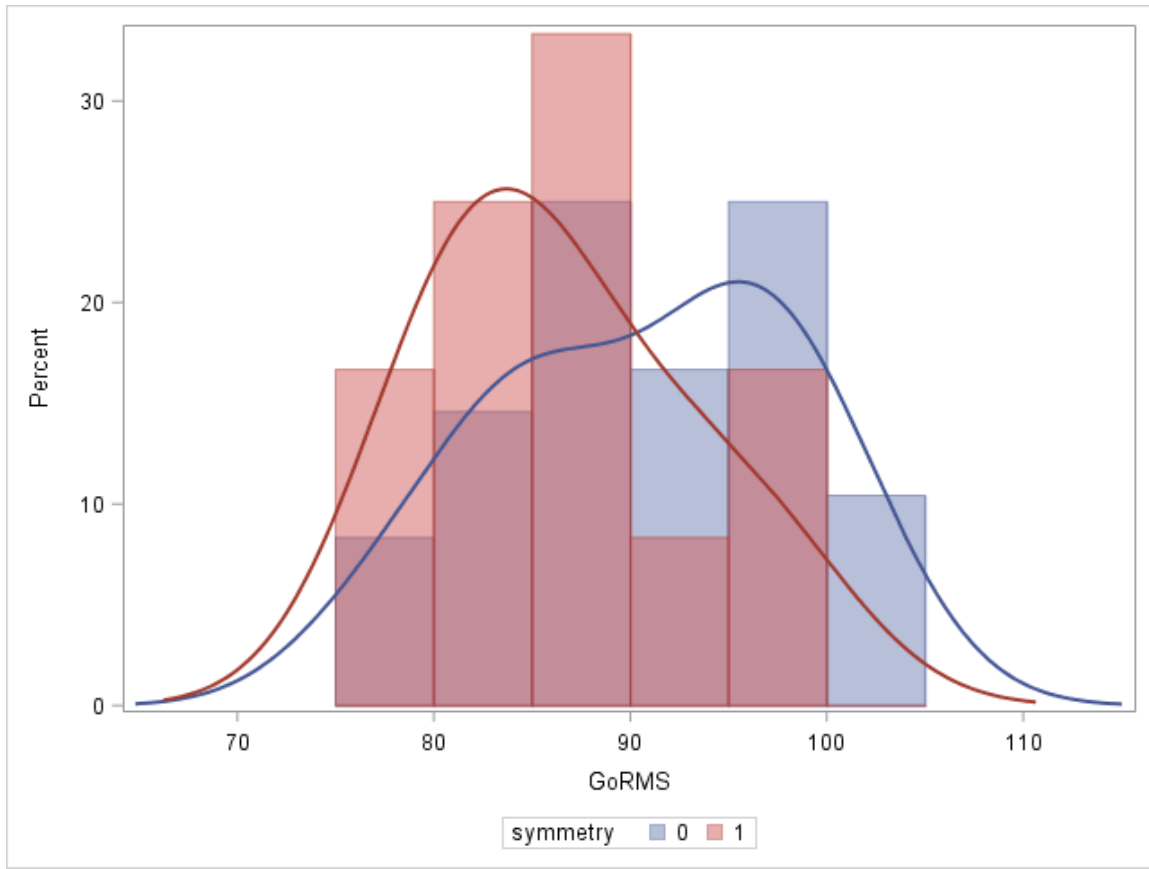


Figure 7. GoR-MS measurements in the symmetric and asymmetric group.

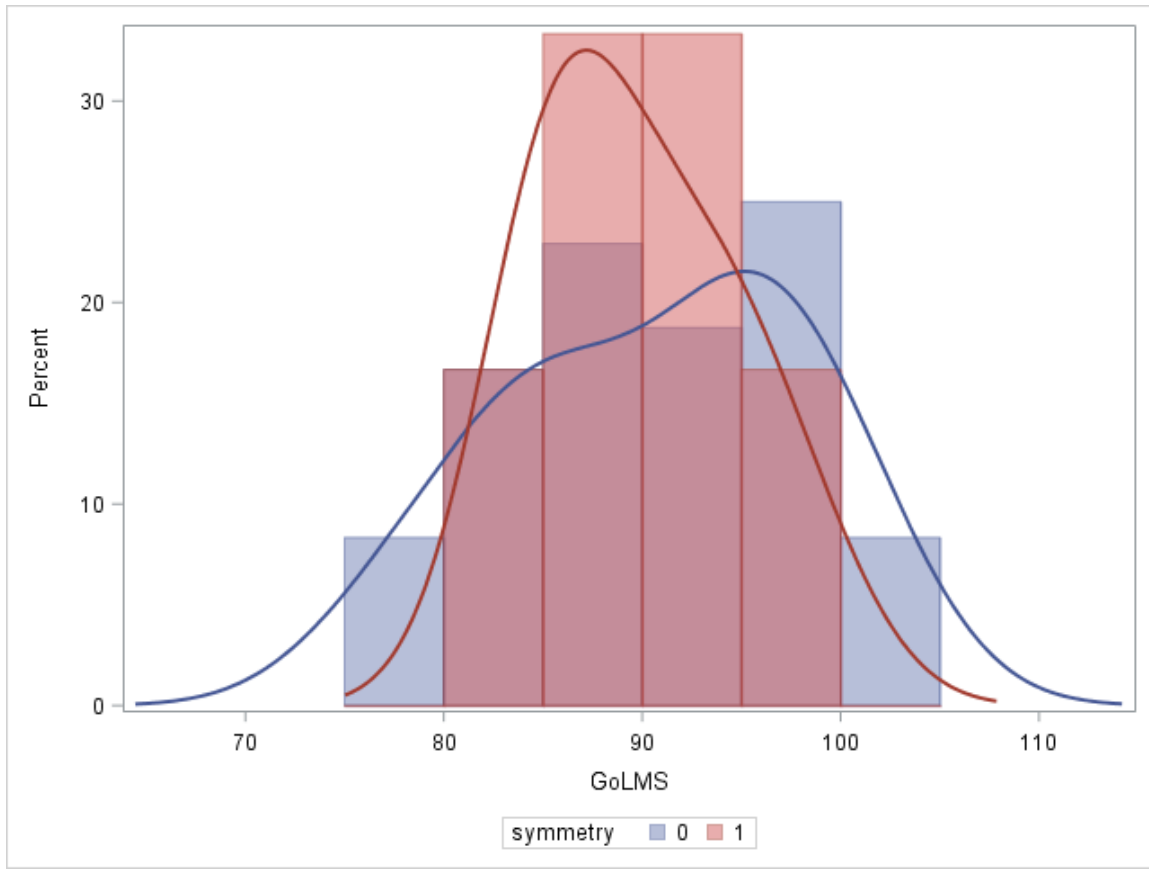


Figure 8. GoL-MS measurements in the symmetric and asymmetric group.

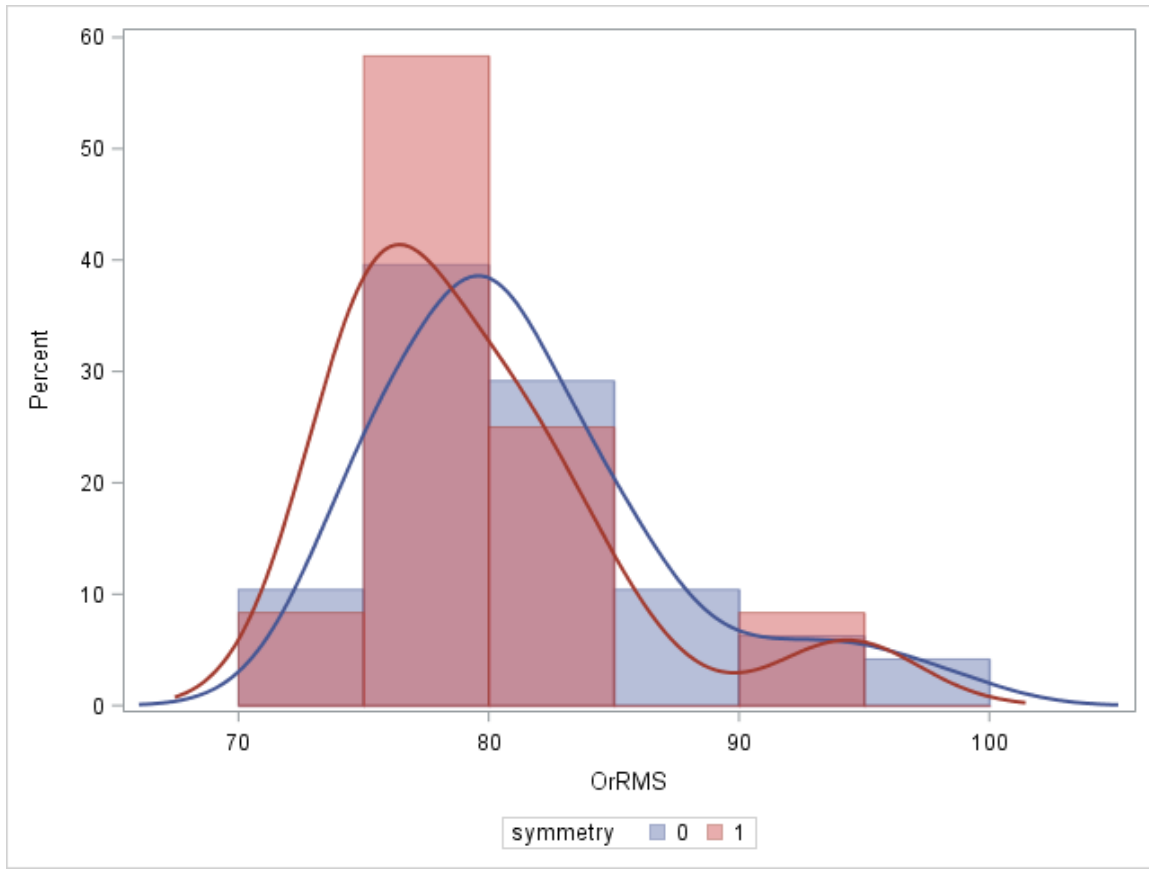


Figure 9. OrR-MS measurements in the symmetric and asymmetric group.

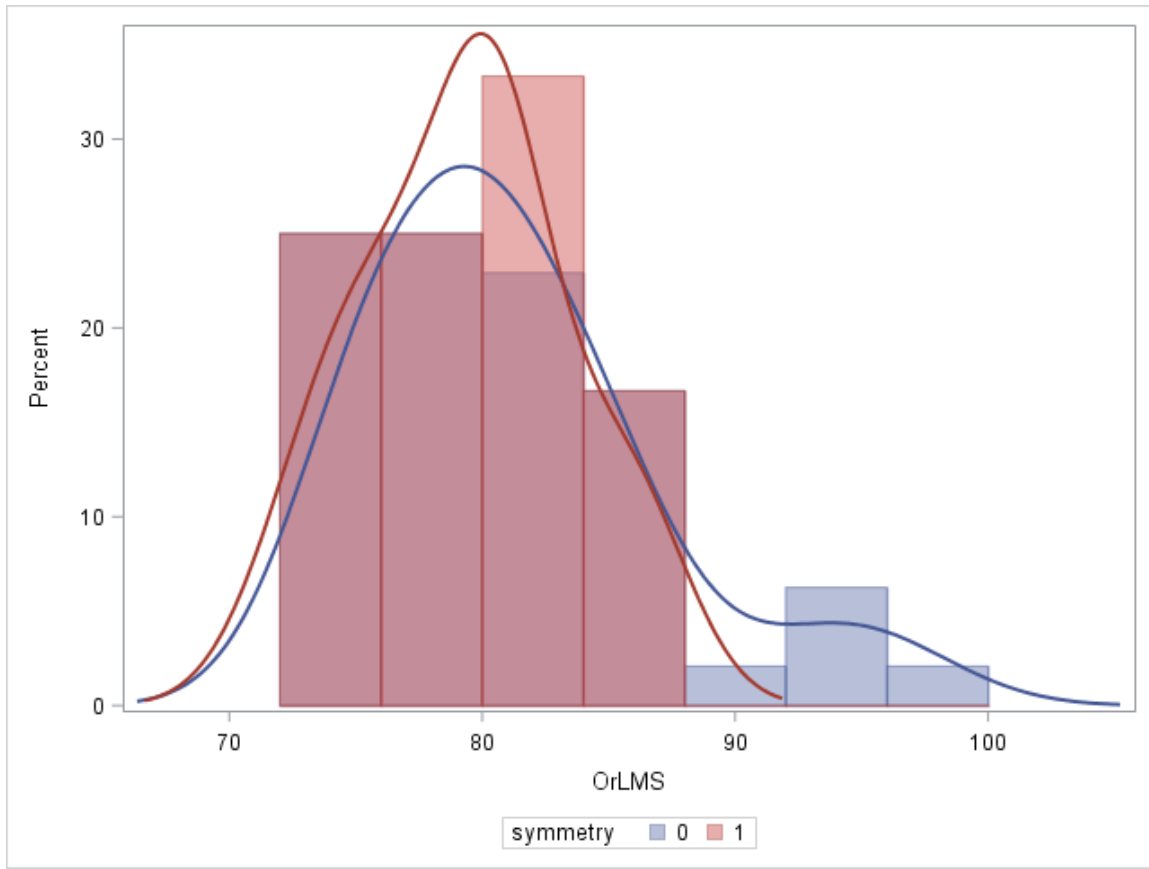


Figure 10. OrL-MS measurements in the symmetric and asymmetric group.

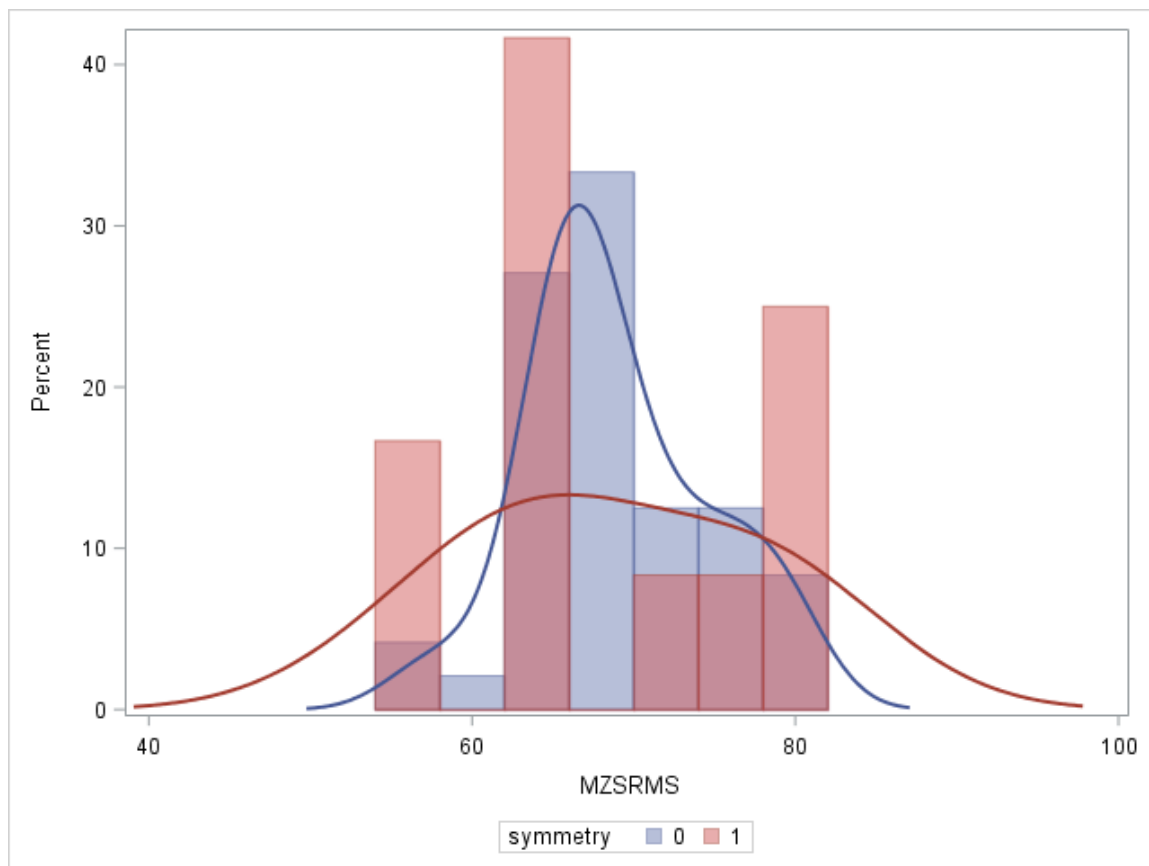


Figure 11. MZSR-MS measurements in the symmetric and asymmetric group.

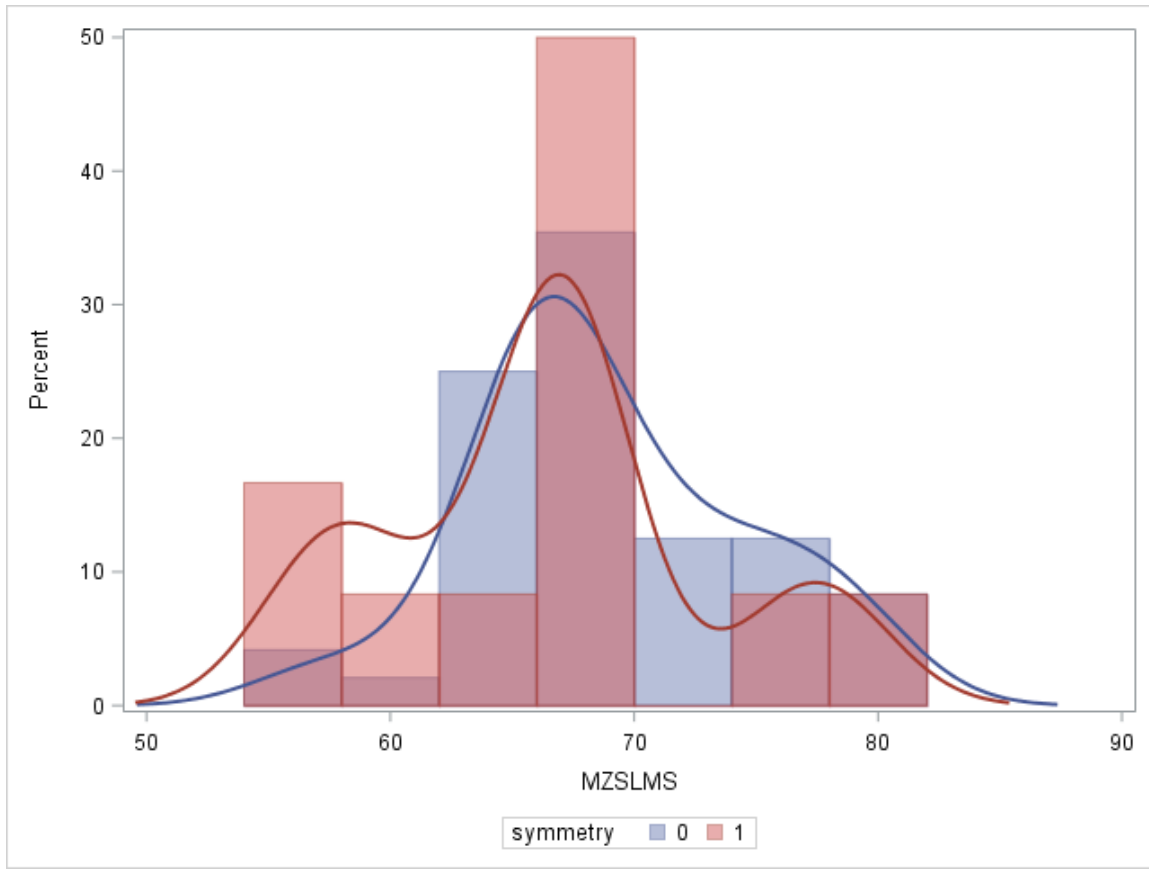


Figure 12. MZSL-MS measurements in the symmetric and asymmetric group.

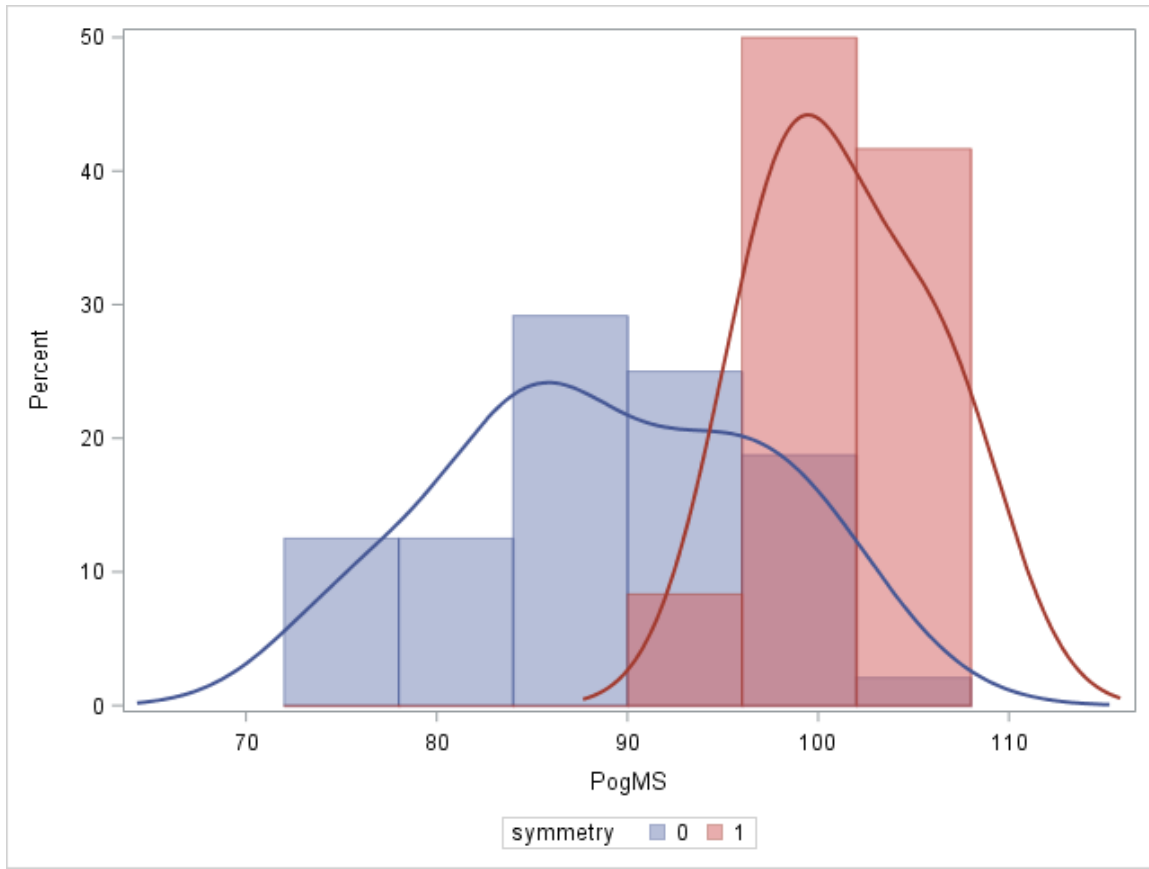


Figure 13. Pog-MS measurements in the symmetric and asymmetric group.

DISCUSSION

The purpose of this study was to investigate correlations between hard and soft tissue images in order to begin to define asymmetry. Three-dimensional images of two groups, symmetric patients and asymmetric patients, were used to locate bilateral and medial anatomic hard tissue and soft tissue landmarks. Linear measurements were recorded in reference to three predetermined reference planes. Our goal was to determine the measurement correlations between hard and soft tissue landmarks to discover where asymmetries originate. Considering the results of this study, statistical significant differences exist in linear measurements between hard and soft tissue points when comparing symmetric and asymmetric subjects. The points that were statistically significant in the three reference planes were Pogonion, Gnathion, and Gonion. Also, statistically significant results show that the correlation between the hard and soft tissue landmarks in symmetric patients is high, particularly in the Mid-Sagittal plane.

A total of 10 hard tissue soft tissue anatomically paired landmarks were chosen for this study. They were chosen for several reasons: based on their distribution throughout skull and face, the assured presence, and their clear visibility on the CBCT scans. Our null hypothesis was there is no statistical significant difference in the location/linear distance between landmark pair positions in the left and right sides of facial skeleton and the soft tissue when measured to 3-dimensional reference planes in symmetric and asymmetric patients. To determine statistical significance, the means of each landmark pair were subjected to either student t-test or Wilcoxon rank sum test (based on the normality of the data) with a 5% significance or p-value of 0.05. In general,

most landmarks did not show statistical significant differences between symmetric and asymmetric subjects among the three planes, as determined by a p-value of greater than 0.05, and thus we accept our null hypothesis.

We did, however, find statistically significant differences in the mean linear measurements between symmetric and asymmetric subjects in three specific landmarks respective to their 3-D reference planes. These landmarks are Pogonion, Gnathion, and Gonion. What is interesting is that the statistical significant measurements amongst the three landmarks are not consistent in all three-reference planes. This is evident when looking at the mean measurement differences in hard and soft tissue Pog, which is significant in the MS and Cor plane, but not in the NH plane. Also, there are inconsistencies between the significance in hard and soft tissue landmarks when comparing the three reference planes. For example, Gn' was statistically significant in both the MS and NH plane, but not in the Cor plane. Furthermore, hard tissue points Gn, GoR and GoL were found significant in the NH plane but not in the other two planes.

A couple of reasons can explain these findings. The first is that asymmetries are truly 3-dimensional and must be defined using 3-dimensional imagery. Significant statistical differences between the symmetric and asymmetric subjects existed in one plane, but not always in all the 3 reference planes. Therefore, if one were viewing the subject simply in 2-dimensions an asymmetry may have been missed or not defined properly. Our landmarks were then given x-, y-, and z- coordinates and measured to reference planes in three dimensions. Not only were our methods to establish landmarks (both hard and soft tissue) and evaluate correlations different, more importantly our imaging modality and analysis were superior and performed using cone beam computed

tomography and the specialized software InVivoDental5.3. Two dimensional analysis of a three dimensional structure, as was previously discussed in the review of literature, has many inherent limitations and does not yield the same accuracy of diagnostic information that we can obtain from a 3D analysis.

Secondly, a total number of 7 soft tissue points were statistically significant, compared to 5 hard tissue points (among the 3 planes). This suggests that soft tissue asymmetries may exist even if there is no underlying hard-tissue asymmetry. Although studies show that there is a clear correlation between the relief of the skull and soft tissue of the face, these results show that this may not always be true, especially in asymmetric patients. Our study showed high correlations between hard and soft tissue points in symmetric patients, especially in the MS plane ($0.92 < r < .99$) with a p value = .0001. And no statistical significance was founded in the asymmetric group. This could suggest more variability in the correlations between hard and soft tissue landmarks in asymmetric patients. In a study by Kim et al, they used 3D CT image analysis with InVivoDental software to collect linear, angular and volumetric cranial base measurements. Statistically significant results were reported in hemi-base volumes being greater on the non-deviated side of asymmetric patients, when compared to symmetric patients²⁷. Kwon et al performed a similar study with contrasting results. They also used 3D CT image analysis but did not find a statistical difference between the symmetric and asymmetric groups, nor within either of the groups²⁵. The conflicting results infer that there is no definitive answer concerning skull and soft tissue asymmetry.

Another valid reason to explain the results of this study is that the number of images in the study's asymmetric group is smaller than the symmetric group (n=12 vs.

n=48), and thus this could have influenced our results in a variety of ways. Perhaps the mean differences would have been even greater if more asymmetric patients were examined, or the mean differences would have been present in more skeletal landmarks if more asymmetric patients were identified. Furthermore, perhaps the correlation tests performed for the asymmetric group would have had different statistical results with a larger sample size. Another limitation of the study is that the index used to originally divide the 60 subjects into “symmetric” and “asymmetric” was based on a 2-dimensional index. A 2-dimensional soft tissue screen capture was used to index the patients and not a 3-dimensional soft tissue drape of the subject.

Moreover, our review of literature discussed the frequencies of asymmetry in the human population. Although the study done subjectively defined asymmetries, it was founded that 74% of asymmetries occur in the lower 1/3 of the face³. Therefore our findings, which show Pog, Go, and Gn as statistically significant, agree with trends of asymmetries founded in the human face thus far. Although these findings are statistically significant, this does not necessarily mean that they are clinically significant. This particular study did not consider a clinical evaluation of the patients, however a 2-dimensional asymmetric index of all images was completed. Thus we assume facial symmetry in the symmetric group was present in these patients and asymmetries in the asymmetric group. However, the asymmetric group was not further divided into smaller groups depending on the location of the asymmetry. Nonetheless, the asymmetry indexing used focused more on the lower 1/3 of the face, and thus it can be assumed the asymmetry group (n=12) had facial asymmetries mostly in this area. However, this tells us two things that may be of clinical significance: the CBCTs images used in the study

confirmed that asymmetries are more common in the lower 1/3 of the face, and hard tissue asymmetries do not necessarily translate to soft tissue asymmetries in asymmetric patients and visa versa.

Although our statistical results and graphical representations provide a useful baseline of measurements, due to the lack of difference in distribution it is difficult for the study to attempt to define where the asymmetries originate. For example, evaluating a larger group of asymmetric patients using the same landmarks and reference planes as in our study can investigate further in finding an origination point of asymmetries in patients. Our methodology can be used to continue to explore the topic and use the graphical distributions to find an actual numerical measurement to determine where the asymmetry originates. Also, an interesting follow up study could be to categorize a sample of patients based on their presenting malocclusion and determine if there is a statistical difference in landmark correlations, that may have a clinical implication in jaw positioning and the resulting occlusion.

CONCLUSIONS

The difference in means of linear measurements of hard and soft tissue landmarks pairs in CBCT images with regards to symmetric and asymmetric subjects revealed non statistical significant results in all landmarks except for six (Pog, Go, Gn, Pog', Go' and Gn'). These landmarks showed statistically significant results, plausible reasons for which were discussed above. Also statistically significant correlation results showed high correlations between hard and soft tissue landmarks in the “symmetric” group.

The future of this pilot study has great potential to begin to further explore asymmetry, as does its three dimensional baseline data for defining asymmetry using reproducible hard and soft tissue landmarks. Further investigation with a larger sample size, utilizing a 3-D asymmetry index, categorizing the sample according to asymmetry location, Angles malocclusion or direct comparison with a discrete sample population, are just some of the potential opportunities for future exploration of this topic.

REFERENCES

1. Rossi, M., Ribeiro, E. & Smith, R. Craniofacial Asymmetry in Development: An Anatomical Study. *Angle Orthod.* **73**, 381–85 (2003).
2. Shah, S. M. & Joshi, M. R. An assessment of asymmetry in the normal craniofacial complex. *The Angle Orthodontist* **48**, 141–148 (1978).
3. Peck, H. & Peck, S. A concept of facial esthetics. *Angle Orthod.* **40**, 284–318 (1970).
4. Peck, S., Peck, L. & Kataja, M. Skeletal asymmetry in esthetically pleasing faces. *The Angle Orthodontist* **61**, 43–48 (1991).
5. Harvold, E. Cleft lip and palate. *Am. J. Orthod.* **40**, 493–506 (1954).
6. Mulick, J. F. An investigation of craniofacial asymmetry using the serial twin-study method. *Am. J. Orthod.* **51**, 112–129 (1965).
7. Letzer, G. & Kronman, J. A posteroanterior cephalometric evaluation of craniofacial asymmetry*. *Angle Orthod.* **37**, 205–211 (1967).
8. VIG, P. S. & HEWITT, A. B. Asymmetry of the Human Facial Skeleton. *Angle Orthod.* **45**, 125–129 (1975).
9. Woo, T. L. On the asymmetry of the human skull, *Biometrika*, Vol. 22:324, 1931, pp. 324-352. *Biometrika* at <http://www.jstor.org/discover/10.2307/2332100?sid=21105737291561&uid=2&uid=4&uid=2134&uid=70>
10. Bjork, A (Professor, D. Odont, Copenhagen, D. Cranial base development a. (1952).

11. Fisher, B. Asymmetries of the Dentofacial Complex. *Angle Orthod.* **24**, 179–92 (1954).
12. Farkas LG. Anthropometry of the head and face. New York: Raven Press. 1994
13. Grammer K, Thornhill R, Human facial attractiveness and sexual selection: the role of symmetry and averageness. *J Comp Psychology.* Sept; 108: 233-42 (1994.)
14. Bishara, S. E., Burkey, P. S. & Kharouf, J. G. Dental and facial asymmetries: a review. *Them Angle Orthodontist* **64**, 89–98 (1994).
15. De Beer, G. De Beer, Gfavin. ‘R. 1937 The development of the vertebrate skull.’ University Proc. Zool. Soc. Lond 289: 61. at <<http://www.sidalc.net/cgi-bin/wxis.exe/?IsisScript=FCL.xis&method=post&formato=2&cantidad=1&expression=mfn=000141>>
16. Lieberman, D. E., Ross, C. F. & Ravosa, M. J. The primate cranial base: ontogeny, function, and integration. *Am. J. Phys. Anthropol.* **Suppl 31**, 117–169 (2000).
17. Lang, J. *Skull Base and Related Structures: Atlas of Clinical Anatomy.* (Schattauer Verlag, 2001). at <<http://books.google.com/books?hl=en&lr=&id=pkY-4NJrC0wC&pgis=1>>
18. Moore, W. & Lavelle, C. Growth of the Facial Skeleton in the Hominoidea. (1974). at <https://scholar.google.com/scholar?hl=en&q=moore+and+lavelle+1974+cranial+base&btnG=&as_sdt=1%2C22&as_sdtp=#0>
19. Scott, J. H. H. The cranial base. *Am J Phys Anthr.* **16**, 319–348 (1958).

20. Enlow, D. H. *Facial growth*. (SPCK Publishing, 1990). at
<[http://books.google.com/books/about/Facial_growth.html?id=a9JqAAAAMAAJ
&pgis=1](http://books.google.com/books/about/Facial_growth.html?id=a9JqAAAAMAAJ&pgis=1)>
21. Laitman, J. T. & Heimbuch, R. C. The basicranium of Plio-Pleistocene hominids as an indicator of their upper respiratory systems. *Am. J. Phys. Anthropol.* **59**, 323–43 (1982).
22. Bastir, M., Sobral, P. G., Kuroe, K. & Rosas, A. Human craniofacial sphericity: a simultaneous analysis of frontal and lateral cephalograms of a Japanese population using geometric morphometrics and partial least squares analysis. *Arch. Oral Biol.* **53**, 295–303 (2008).
23. Burke, P. . Stereophotogrammetric measurement of normal facial asymmetry in children. *Hum. Biol.* **43**, 536–548 (1971).
24. Arnold, T. G., Anderson, G. C. & Liljemark, W. F. Cephalometric norms for craniofacial asymmetry using submental-vertical radiographs. *Am. J. Orthod. Dentofacial Orthop.* **106**, 250–6 (1994).
25. Kwon, T.-G., Park, H.-S., Ryoo, H.-M. & Lee, S.-H. A comparison of craniofacial morphology in patients with and without facial asymmetry--a three-dimensional analysis with computed tomography. *Int. J. Oral Maxillofac. Surg.* **35**, 43–8 (2006).
26. Baek, S.-H., Cho, I.-S., Chang, Y.-I. & Kim, M.-J. Skeletodental factors affecting chin point deviation in female patients with class III malocclusion and facial asymmetry: a three-dimensional analysis using computed tomography. *Oral Surg. Oral Med. Oral Pathol. Oral Radiol. Endod.* **104**, 628–39 (2007).

27. Kim, S.-J., Lee, K.-J., Lee, S.-H. & Baik, H.-S. Morphologic relationship between the cranial base and the mandible in patients with facial asymmetry and mandibular prognathism. *Am. J. Orthod. Dentofacial Orthop.* **144**, 330–40 (2013).
28. Grayson, B., Cutting, C., Bookstein, F. L., Kim, H. & McCarthy, J. G. The three-dimensional cephalogram: Theory, techniques, and clinical application. *Am. J. Orthod. Dentofac. Orthop.* **94**, 327–337 (1988).
29. Swennen, G. R. J. *et al.* Three- Dimensional cephalometry: a color atlas and manual. New York, NY Springer. 2005
30. Captier, G. *et al.* Plagiocephaly: morphometry of skull base asymmetry. *Surg. Radiol. Anat.* **25**, 226–33
31. Berco, M. *et al.* Accuracy and reliability of linear cephalometric measurements from cone-beam computed tomography scans of a dry human skull. *Am. J. Orthod. Dentofacial Orthop.* **136**, 17.e1–9; discussion 17–8 (2009).
32. You, K.-H., Lee, K.-J., Lee, S.-H. & Baik, H.-S. Three-dimensional computed tomography analysis of mandibular morphology in patients with facial asymmetry and mandibular prognathism. *Am. J. Orthod. Dentofacial Orthop.* **138**, 540.e1–8; discussion 540–1 (2010).
33. Katsumata, A. *et al.* 3D-CT evaluation of facial asymmetry. *Oral Surg. Oral Med. Oral Pathol. Oral Radiol. Endod.* **99**, 212–20 (2005).
34. Lascala, C. A., Panella, J. & Marques, M. M. Analysis of the accuracy of linear measurements obtained by cone beam computed tomography (CBCT-NewTom). *Dentomaxillofac. Radiol.* **33**, 291–4 (2004).

35. Lagravère, M. O., Carey, J., Toogood, R. W. & Major, P. W. Three-dimensional accuracy of measurements made with software on cone-beam computed tomography images. *Am. J. Orthod. Dentofacial Orthop.* **134**, 112–6 (2008).
36. Swennen, G. R. J. & Schutyser, F. Three-dimensional cephalometry: Spiral multi-slice vs cone-beam computed tomography. *Am. J. Orthod. Dentofac. Orthop.* **130**, 410–416 (2006).
37. Miracle, A. C. & Mukherji, S. K. Conebeam CT of the head and neck, part 1: physical principles. *AJNR. Am. J. Neuroradiol.* **30**, 1088–95 (2009).
38. Miracle, A. C. & Mukherji, S. K. Conebeam CT of the head and neck, part 2: clinical applications. *AJNR. Am. J. Neuroradiol.* **30**, 1285–92 (2009).
39. Parsi, K. G. Morphometric analysis of facial and skeletal structures and its relationship to attractiveness- A three dimensional analysis. (Boston University, 2014).
40. Baccetti, T., Franchi, L. & McNamara, J. a. An Improved Version of the Cervical Vertebral Maturation (CVM) Method for the Assessment of Mandibular Growth. *Angle Orthod.* **72**, 316–323 (2002).
41. Angelopoulos, C. Cone beam tomographic imaging anatomy of the maxillofacial region. *Dent. Clin. North Am.* **52**, 731–52, vi (2008).
42. *Cone Beam CT and 3D imaging.* (Springer Milan, 2014). doi:10.1007/978-88-470-5319-9
43. Moss, M. & Salentijn, L. Differences between the functional matrices in anterior open-bite and in deep overbite. *Am. J. Orthod.* (1971). at <<http://www.sciencedirect.com/science/article/pii/0002941671901357>>

44. Forsberg, C. T., Burstone, C. J. & Hanley, K. J. Diagnosis and treatment planning of skeletal asymmetry with the submental-vertical radiograph. *Am. J. Orthod.* **85**, 224–237 (1984).
45. Brash, J. & McKeag, H. The aetiology of irregularity and malocclusion of the teeth. (1956). at
https://scholar.google.com/scholar?hl=en&q=brash+1956+&btnG=&as_sdt=1%2C22&as_sdt=#0
46. CHEBIB, F. S. & CHAMMA, A. M. Indices of Craniofacial Asymmetry. **51**, 214–226 (1981).
47. Ritucci, R. & Burstone, C. Use of the submental vertical radiograph in the assessment of asymmetry. *Thesis* (1981). at
https://scholar.google.com/scholar?hl=en&q=ritucci+and+burstone+asymmetry&btnG=&as_sdt=1%2C22&as_sdt=#2
48. Marmary, Y., Zilberman, Y. & Mirsky, Y. Use of foramina spinosa to determine skull midlines. *Angle Orthod.* (1979). at
[http://www.angle.org/doi/pdf/10.1043/0003-3219\(1979\)049%3C0263:UOFSTD%3E2.0.CO%3B2](http://www.angle.org/doi/pdf/10.1043/0003-3219(1979)049%3C0263:UOFSTD%3E2.0.CO%3B2)
49. Silva, M. A. G. *et al.* Cone-beam computed tomography for routine orthodontic treatment planning: a radiation dose evaluation. *Am. J. Orthod. Dentofacial Orthop.* **133**, 640.e1–5 (2008).
50. Lou, L., Lagravere, M. O., Compton, S., Major, P. W. & Flores-Mir, C. Accuracy of measurements and reliability of landmark identification with computed

- tomography (CT) techniques in the maxillofacial area: a systematic review. *Oral Surg. Oral Med. Oral Pathol. Oral Radiol. Endod.* **104**, 402–11 (2007).
51. Ludlow, J. B., Laster, W. S., See, M., Bailey, L. J. & Hershey, H. G. Accuracy of measurements of mandibular anatomy in cone beam computed tomography images. *Oral Surg. Oral Med. Oral Pathol. Oral Radiol. Endod.* **103**, 534–42 (2007).
52. Hilgers, M. L., Scarfe, W. C., Scheetz, J. P. & Farman, A. G. Accuracy of linear temporomandibular joint measurements with cone beam computed tomography and digital cephalometric radiography. *Am. J. Orthod. Dentofac. Orthop.* **128**, 803–811 (2005).
53. Kreiborg, S. *et al.* Comparative three-dimensional analysis of CT-scans of the calvaria and cranial base in Apert and Crouzon syndromes. *J. Cranio-Maxillofacial Surg.* **21**, 181–188 (1993).
54. Grauer, D., Cevidanes, L. S. H. & Proffit, W. R. Working with DICOM craniofacial images. *Am. J. Orthod. Dentofacial Orthop.* **136**, 460–70 (2009).
55. Chien, P. *et al.* Comparison of reliability in anatomical landmark identification using two-dimensional digital cephalometrics and three-dimensional cone beam computed tomography in vivo. *Dentomaxillofacial Radiol.* **38**, 262–273 (2009).
56. Muramatsu, A. *et al.* Reproducibility of Maxillofacial Anatomic Landmarks on 3-Dimensional Computed Tomographic Images Determined with the 95% Confidence Ellipse Method. *Angle Orthod.* **78**, 396–402 (2008).

57. Gribel, B., Gribel, M. & Frazão, D. Accuracy and reliability of craniometric measurements on lateral cephalometry and 3D measurements on CBCT scans. *Angle ...* (2011). at <<http://www.angle.org/doi/abs/10.2319/032210-166.1>>
58. Schulze, R. *et al.* Artefacts in CBCT: a review. *Dentomaxillofac. Radiol.* **40**, 265–73 (2011).
59. Scarfe, W. C. & Farman, A. G. What is cone-beam CT and how does it work? *Dent. Clin. North Am.* **52**, 707–30, v (2008).
60. De Vos, W., Casselman, J. & Swennen, G. R. J. Cone-beam computerized tomography (CBCT) imaging of the oral and maxillofacial region: a systematic review of the literature. *Int. J. Oral Maxillofac. Surg.* **38**, 609–25 (2009).

List of Journal Title Abbreviations

Am. J. Neuroradiol.....	American Journal of Neuroradiology
Am. J. Orthod. Dentofacial Orthop.....	American Journal of Orthodontics and Dentofacial Orthopedics
Am. J. Phys. Anthropol.....	American Journal of Physical Anthropology
Angle Orthod	The Angle Orthodontist
Dent Clin North Am.....	Dental Clinics of North America
Hum. Biol.....	American Journal of Human Biology
Int J Oral Maxillofac Surg	International Journal of Oral and Maxillofacial Surgery
J Comp Psychology.....	Journal of Comparative Psychology
J. Cranio-Maxillofacial Surg.....	Journal of Cranio-Maxillofacial Surgery
Oral Surg. Oral Med. Oral Pathol. Oral Radiol. Endod. Oral Surgery, Oral Medicine, Oral Pathology, and Oral Radiology	
Surg. Radiol. Anat.....	Surgical Radiologic Anatomy

CURRICULUM VITAE

